TELKOMNIKA, Vol. 11, No. 7, July 2013, pp. 3718~ 3727
e-ISSN: 2087-278X

Chemical Source Localization using Mobile Robots in Indoor Arena

Yuli Zhang*[1,2], Xiaoping Ma[1], Yanzi Miao[1]
[1]School of Information and Electrical Engineering, China University of Mining and Technology, Xuzhou, China
[2]School of Science, Dalian Jiao Tong University, Dalian, China
Corresponding author, e-mail: zhangyuli1021@hotmail.com, xpma@cumt.edu.cn, miaoyanzi81@163.com

Abstract

This paper presents a virtual-physics force based control strategy for swarm robotic chemical source localization. The control force includes: structure formation force, goal force, and obstacle avoidant force. For swarm formation, the robots maintain the regular polygon formation and a virtual robot is located at the center of the polygon. The motion of the virtual robot depends on the goal force which obtained from the sensor observations of the robots. Once the virtual robot moved to a new place, the robots would also move as a single body with the structure formation force and obstacle avoidant force. In this paper, we adopted chemotaxis as plume tracing algorithms. Simulation experiments in indoor arena without obstacle and with obstacles using different robot number are carried out respectively, and the results show that the proposed strategy can effectively navigate the mobile robotics swarms to the chemical source once selecting proper number of robots.

Keywords*: virtual-physics force, plume tracing, source localization, source identification*

1. Introduction

The recent increasing threat of chemical agents that are accidentally or deliberately released into an environment has highlighted the need for superior detection of chemical emission sources. To minimize damage from chemical agents, we must locate the origin of the chemical as quickly as possible. Because the chemical is often hazardous to human health, a promising solution is to deploy a group of intelligent robots, so that they can autonomously trace the toxic plume to its source emitter, without endangering the lives of human operators. This paper represents a cooperative search strategy based on mobile robotics swarms with virtual-physics force, which can rapidly converge on the location of the source emitter.

Typical strategies and methods designed for plume tracking and source localization include gradient-following-based strategy [1, 2], imitation of animal behavior [3, 4], probabilistic models based on Bayesian occupancy grid mapping [5, 6] and multiple robots cooperation based on swarm intelligence [7, 8], based on evolutionary [9, 10] and by fusing vision information [11, 12]. Zarzhitsky et al. [13] proposed a cooperative group of robots moving in a close formation, also using fluid-dynamics information. Hayes et al. [14] described a spiral surge algorithm in which a collection of autonomous mobile robots used a combination of spiral, surge, and spiral casting behaviors to find the source of an odor plume. Cui et al. [15] had developed a fuzzy logic based approach to control a swarm of small robots to locate a hazardous contaminant source. Jatmiko et al. [16] presented an algorithm for odor source localization in a changing environment based on the particle swarm optimization.

In this paper, we propose a cooperative search strategy using the lattice formations, built with virtual physics force (VPF), as a distributed sensor and computation network that acts as a parallel computer to assist in the making of navigational decisions.

2. Research Method

2.1. Construction of Dynamic Plume Model in Indoor Arena

The plume models that available for mobile robot study and research have many limitations: mostly are the long time average static model in open outdoor arena and no

Received December 19, 2012; Revised April 12, 2013; Accepted April 25, 2013

considering the effect of boundary condition of walls and obstacles. The plume model used in the paper is obtained from Liu [17]. This plume was simulated using a computation fluid dynamic (CFD) software package, FLUENT (Fluent, Inc.). The plume data produced by Fluent CFD were imported into MATLAB (Mathworks, Inc.) and integrated with simulated mobile robots model for pluming tracing behavior simulation. Firstly, the size and the geometry of the indoor simulation arena are defined using Gambit (Fluent Inc.), which is a pre-processor for Fluent. The indoor simulation arena we used in the paper was a 2D arena of 20m×20m with two windows (airflow inlet), a door (airflow outlet). The geometry details of simulation domain are illustrated in Figure 1. Varying airflow directions were adopted instead of the fixed airflow direction, the varying airflow entered into the windows of the indoor simulation domain at a constant 5m/s velocity but varied between ±22.5º during the simulation.

The gas in this paper was Methane (CH_4) with position (2, 14). We constructed two kinds of indoor simulation arena: one has no obstacle, which is given in Figure 1 (a) and the other has three obstacles with (6.75±0.75, 12.75±0.75); (11±1, 8.5±2.5); (13.5±1.5, 15±1) as their vertices, which is shown in Figure 1 (b), to block the odor plume propagation and the robot motions. Plume data (CH_4 concentration, airflow vectors) were calculated by running FLUENT and were stored in files for further processing. FLUENT is one kind of CFD software good at calculation, however, it is not good at post-processing simulation data. In order to obtain a more realistic plume model, we adopted OPENDX to visualize the simulation data. Figure 2 shows two kinds of dynamic CH_4 plume model in indoor arena without obstacle and three obstacles (the rectangular white blocks).

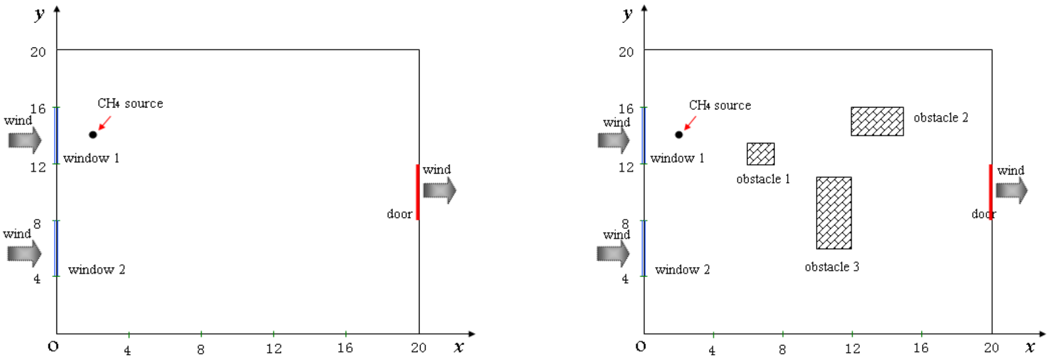

(a) Indoor arena without obstacle (b) Indoor arena with three obstacles

Figure 1. Two dimensional sizes in the indoor arena

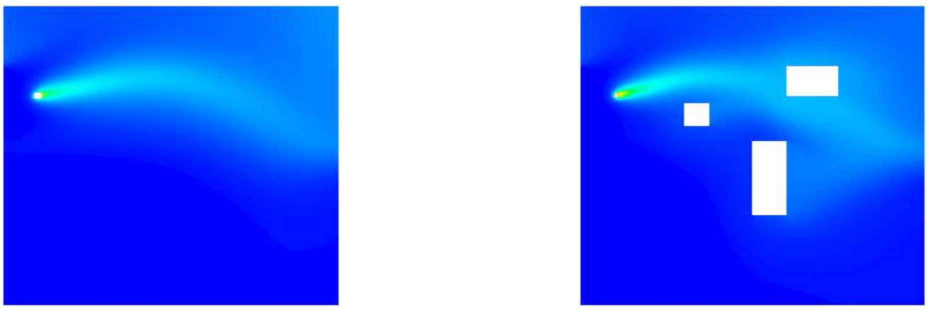

(a) Indoor arena without obstacle (b) Indoor arena with three obstacles

Figure 2. Instantaneous distribution of plume in the indoor arena.

From Figure 2 we can see, the obstacles make the distribution of the plume more diversified.

An advantage of using CFD numerical simulation is that it can simulate plumes precisely; a disadvantage is that we cannot simulate a mobile robot in CFD simulation arena. So the plume data were then imported into MATLAB for integration with the simulated mobile robots model.

2.2. A Virtual Physics-Based Approach to Chemical Source Localization Using Mobile Robots

Virtual physics (VP) provides a distributed control of mobile robots in sensor network. We use the term "virtual physics" because although these forces are defined only inside the control software, the robots act as though the forces are real. Every robot observes the environment, notes the position of nearby robots, and then computes virtual forces imposed upon it. After taking a vector sum of all forces on the robot, it takes derivatives to convert the net force into a velocity vector for the robot's next move. At an abstract level, VP treats agents as physical particles. Each particle *i* has position *X* and velocity *v*. We use a discrete-time approximation to the continuous behavior of the system, with time-step Δt. At each time step, the position of each particle undergoes a perturbation ΔX. The perturbation depends on the current velocity *v*, i.e., $\Delta X = v\Delta t$. The velocity of each particle at each time step also changes by Δv. The change in velocity is controlled by the force on the particle, i.e., $\Delta v=F\Delta t/m$. where *m* is the mass of that particle and *F* is the force on that particle. Generally, the control force includes three kinds of effort, which are virtual structure force *F* (*VS*), virtual goal force *F* (*VG*), and obstacle avoidant force *F* (*OA*). Then taking a vector sum of all forces, i.e., *F=F* (*VS*) +*F* (*VG*) +*F* (*OA*), it converts the net force into a velocity vector for the robot's next move.

F (*VS*) is always a function of distance between the neighboring robots, and does not depend on time. On the other hand, *F* (*VG*) is responsible for directing the swarm toward a goal location, and therefore is computed using the sensor data available on robot *i* at time *t*.

2.2.1. Virtual Structure Force

The virtual structure force *F* (*VS*) as a function of distance between the neighboring robots was defined by Newton's Law of universal gravitation in [13]. Six usual structures corresponding to different robot numbers on the basis of Newton's Law of universal gravitation are illustrated in Figure 3.

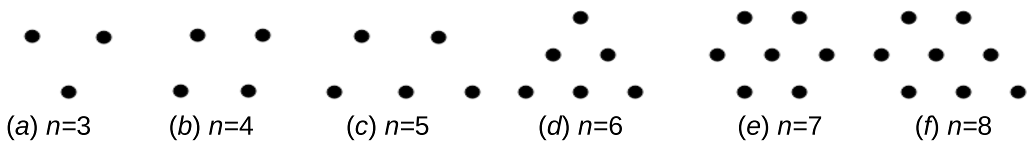

Figure 3. Six usual formations with different robot number *n* in [13]

This paper adopted structure force in [18], which making the robotic swarms keep a regular polygon formation. The input force $(F'_{xk}(VS), F'_{yk}(VS))$ to the *K*-th (*k*=1, 2, 3, …, *n*) robot for regular polygon formation based on the virtual structure can be stated as follows:

$$\begin{cases} F'_{xk}(VS) = \sum_{i=1, i\neq k}^{6} k_r \frac{q_k q_i}{d_{ki}^2}\cos(\theta_{ki}) - k_s(x_k - x_c)((x_k - x_c)^2 + (y_k - y_c)^2 - r^2) \\ F'_{yk}(VS) = \sum_{i=1, i\neq k}^{6} k_r \frac{q_k q_i}{d_{ki}^2}\sin(\theta_{ki}) - k_s(y_k - y_c)((x_k - x_c)^2 + (y_k - y_c)^2 - r^2) \end{cases} \quad (1)$$

where k_r, k_c are positive gain, q_k and q_i are the *K*-th and *i*-th electric charges ($q_k= q_i =1$ in this paper), and d_{ki} is the distance between them, (x_k,y_k) is the position of robot *k*. $\cos(\theta_{ki}) = \frac{x_k - x_i}{|d_{ki}|}, \sin(\theta_{ki}) = \frac{y_k - y_i}{|d_{ki}|}$.

The force defined in (1) makes the robot move toward the circle with center (x_c, y_c) and radius *r* when (x_k, y_k) ≠ (x_c, y_c) and form a regular polygon.

We obtained united vector as follows:

$$(F_{xk}(VS), F_{yk}(VS)) = \frac{(F'_{xk}(VS), F'_{yk}(VS))}{\left\|(F'_{xk}(VS), F'_{yk}(VS))\right\|} \quad (2)$$

Six usual structures corresponding to different robot numbers on the basis of virtual structure force (F_{xk} (*VS*), F_{yk} (*VS*)) are illustrated in Figure 4.

(a) *n*=3 (b) *n*=4 (c) *n*=5 (d) *n*=6 (e) *n*=7 (f) *n*=8

Figure 4. Six usual formations with different robot number *n* in [18]

Comparing Figure 3 with Figure 4, we can see the formation in Figure 4 has a wider distribution than it in Figure 3 under the same condition of the robots' number and adjacent distance between robots. The robots in formation of Figure 4 can sense a larger range of data. So we adopted the formation of Figure 4 in this paper. For swarm formation of the robots, a virtual robot is considered at the center of the circle while the robots are placed on the circle around it. Therefore, (x_c, y_c) in (1) should be replaced by (x_v, y_v) that is the coordinate of the virtual robot. In this paper, the virtual robot was considered as a leader who received the sensor data available on robot *k* (*k*=1, 2, 3… *n*), processed the data and made the motion decision.

2.2.2. Virtual Goal Force

In this paper, we discussed chemical source localization in indoor area. Firstly, we placed the robots at the vicinity of the entrance (door), and with the virtual structure force (F_{xk} (*VS*), F_{yk} (*VS*), the robots formed a regular polygon shown as Figure 4. If the gas concentrations some robots sensed exceeded a predefined threshold ρ_T the robots used gradient strategy to trace the gas plume. The gradient strategy simply follows the chemical gradient, so the direction of the largest chemical concentration is the goal direction. We put the virtual goal force only on virtual robot. The virtual received the sensor data available on robot k (*k*=1, 2, 3, …, *n*), choose the robot *j* who had the highest concentration and moved toward it a distance of step length s_1. The virtual force is defined as follows：

$$F(VG)=\frac{X_j(t)-X_v(t)}{\left\|X_j(t)-X_v(t)\right\|} \quad (3)$$

where X_v and X_j are position of virtual robot and robot *j*. ‖•‖represents the Euclidean norm operator.

Then, the discrete-time model of the virtual robot movements can be stated as:

$$X_v(t+1)=X_v(t)+s_1\cdot F(VG) \quad (4)$$

where X_v (t+1) and X_v (t)are position of the virtual robot at time step *t*+1 and *t*. As the virtual robot moved to a new position, the robots would also move a distance of step length s_2 under the action of the virtual structure force. So, the robots move as a polygon formation.

So, the discrete-time model of the robot movements can be stated as:

$$X_k(t+1)=X_k(t)+s_1\cdot F_k(VS) \quad (5)$$

where X_k (t+1) and X_k (t) are position of the robot *k* (*k*=1, 2, 3, … , *n*) at time step *t*+1 and *t*.
It should be noted that step length s_1 of the virtual robot should less than that of the robots such that the robots can follow it.

2.2.3. Obstacle Avoidance Force

Because robots have a physical shape and foot print of finite size, and cannot have intersecting trajectories. Thus, robots must avoid collisions with other robots in addition to avoiding obstacles in the environment. In this paper, we adopted the simple reactive wall-following obstacle avoidance method which requires less computation and does not require a prior knowledge of the environment and past history of robot navigation. The robot in this study was equipped with five ultrasonic sensors, as each ultrasonic sensor covered a 36º angle; five sensors covered totally 180º area in front of this robot which is enough for the robot to detect objects at the front. The configuration of ultrasonic sensors is illustrated in Figure 5.

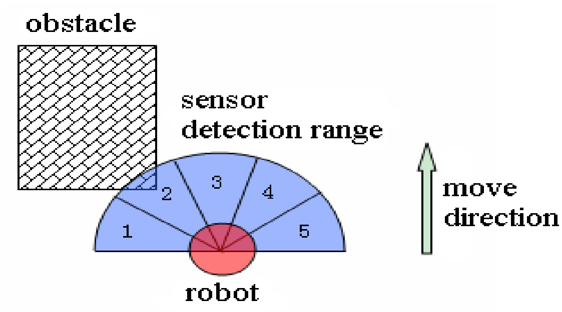

Figure 5. Configuration of the ultrasonic sensors of the robot

Based on the sensory information from the ultrasonic sensors, if the robot detects an object within its alarm distance, it implements avoidance force to adjust the move direction to detour around that object until no obstacles are detected and then the robot will continue moving forward. The obstacle avoidance force is defined bellow.
Let D the distance readings from the five ultrasonic sensors:

$$D = \{d_i(t)\}, i = 1,2,3,4,5 \tag{6}$$

where $d_i(t) = \begin{cases} 1, & d_i(t) < d_0 \\ 0, & otherwise \end{cases}$ and d_0 is alarm distance.

The deflection angle of the move direction of the robot θ_b is defined as follows:

$$\theta_b = \begin{cases} -90^\circ & d_3(t) = 1 \\ -30^\circ & d_2(t) = 1 \; and \; d_3(t) = 0 \\ -15^\circ & d_1(t) = 1 \; and \; d_2(t) = 0 \; and \; d_3(t) = 0 \\ 30^\circ & d_4(t) = 1 \; and \; d_3(t) = 0 \\ 15^\circ & d_5(t) = 1 \; and \; d_4(t) = 0 \; and \; d_3(t) = 0 \\ 0 & otherwise \end{cases} \tag{7}$$

Let $\tilde{\theta}$ the include angle between $F_k(VS)$ (k=1, 2, 3, … , n) to the K-th (k=1, 2, 3, … , n) robot and positive axis of x, then the virtual structure force ($F_{xk}(VS)$, $F_{yk}(VS)$) to the K-th (k=1, 2, 3, … , n) robot will be modified by:

$$\begin{cases} F''_{xk}(VS) = F_k(VS)\cos(\tilde{\theta} + \theta_b) \\ F''_{yk}(VS) = F_k(VS)\sin(\tilde{\theta} + \theta_b) \end{cases} \tag{8}$$

Then obstacle avoidance force is defined as follows:

$$\begin{cases} F_{xk}(OA) = F''_{xk}(VS) - F_{xk}(VS) \\ F_{yk}(OA) = F''_{yk}(VS) - F_{yk}(VS) \end{cases} \tag{9}$$

Obviously, if the surroundings of the robot are clear, the obstacle avoidance force is 0 and the virtual structure force $(F''_{xk}(VS), F''_{yk}(VS))$ is restored to $(F_{xk}(VS), F_{yk}(VS))$.

So, the discrete-time model of the robot movements can be stated as:

$$X_k(t+1) = X_k(t) + s_1 \cdot F_k''(VS) \quad (10)$$

where X_k (t+1) and X_k (t) are position of the robot k (k=1, 2, 3, … , n) at time step t+1 and t.

2.2.4. Source Declaration

Plume source identification is the process whereby the robots identify the odor source in the environment. It is found that, an important characteristic of the odor source is preserving a high concentration in a long time. In this paper, when arriving at the emitter region, because of the balance of the inner structure force and external goal force, the robots get bogged down and become a circle surrounding the potential source emitter. If the maximum gas concentration of the robot sensor in the robots is greater than a given threshold Φ_T in a given number of steps n_s, we decide that the odor source is located and the robots stops automatically.

3. Results and Analysis

The virtual physics-based approach to chemical source localization we adopted was tested in indoor dynamic plume arena which was shown in Figure 2. At the same time, we gave the search results with the different number of robots.

3.1. The Parameters of the Algorithm

By simulating extensive numerical search trials for each parameter, we chose the parameter given by Table 1.

Table 1. Parameters of algorithm

k_c	r	k_r	s_1	s_2	ρ_T	d_0	Φ_T	n_s
0.0001	0.3	5	0.06	0.12	0.0095	0.8	0.1	5

3.2. Performance Metrics

We gave the following three performance metrics:

Success rate : the percentage of trials in which the robots found the plume source;
Search time : the total length of time that the robots fund the plume source;
Overall proximity : a measure of how close the virtual robot was to the CH_4 source during the simulation run.

Firstly, we give the simulation result in the indoor arena without obstacle.

3.3. Simulation Result in the Indoor Arena without Obstacle

To get a better understanding of the effect that the control algorithm has on the plume tracing task, we give a series of snap shots of the tracing odor plumes process of the six robots in the indoor arena without obstacle (see Figure 6).

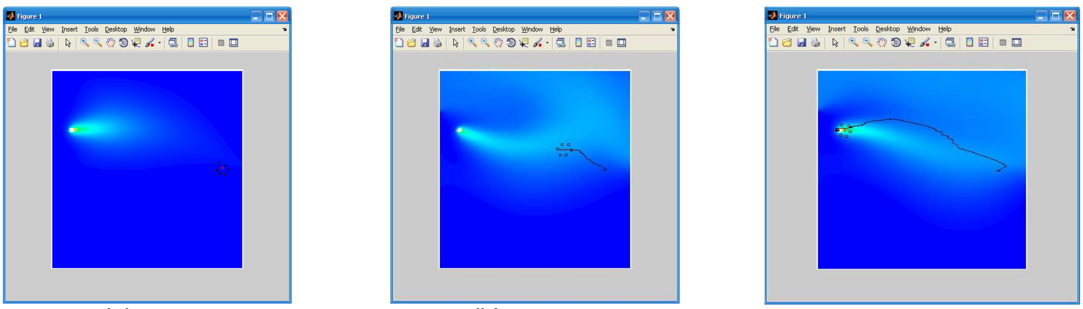

(a) t=3s (b) t=100s (c) t=382s

Figure 6. The virtual physics-based plume tracing process in indoor arena without obstacle

At the beginning, six robots (indicated by "○") and a virtual robot (indicated by "+") are distributed randomly in the entrance area. At the time t=3s (see Figure 6(a)), the structure force defined in (1) makes the robots to provide a hexagonal structure. Once some of the robots detect the plume, the robots trace the plume to its source with the control algorithm while preserving a stable hexagonal structure (see Figure 6(b)). At last, the robots find the source and the search is end (see Figure 6(c)).

Figure 7 and Figure 8 show the search results with the different number of robots *n* in the indoor arena without obstacle. In order to more clearly display the effect of the robots tracing plume, Figure 7 only gives a tracing path of one of the robots. Figure 8 shows the search time and the overall proximity of the robots.

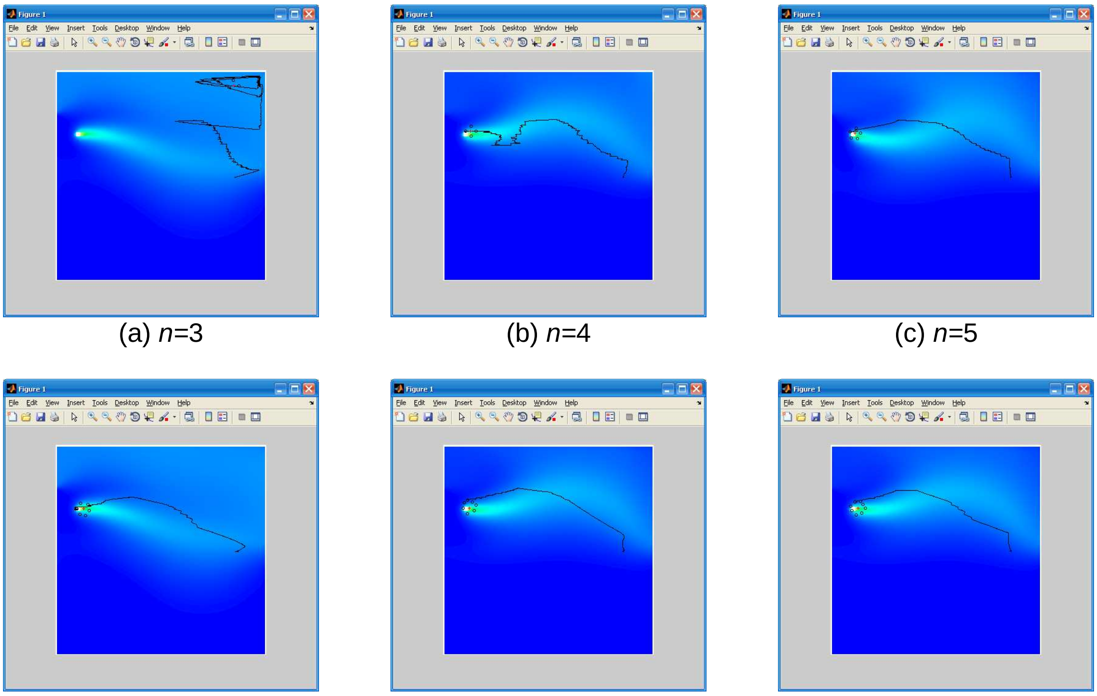

(a) *n*=3 (b) *n*=4 (c) *n*=5

(d) *n*=6 (e) *n*=7 (f) *n*=8

Figure 7. Plume tracing path using the virtual physics in indoor arena without obstacle with different robot number *n*

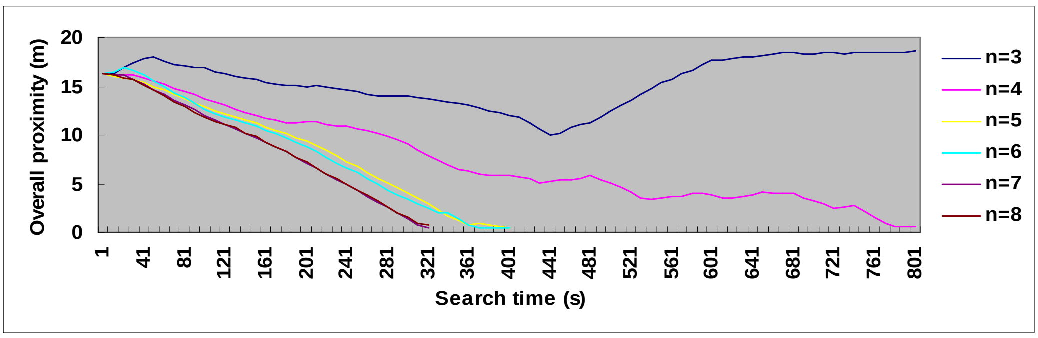

Figure 8. The performance of plume tracing using the virtual physics in indoor arena without obstacle with different robot number n

From Figure 7 and Figure 8 we can see that when the robot number is smaller, the sensor data from the robots is limited, and so the search time of the robots is longer. Especially when the robot number is 3, the robots fall into the plume swirls which on the top right corner of the simulation area and cannot escape it which leading the search failed. When the robot number is more than 4, the tracing path of the robots is very similar to each other with different robot number *n* and the search time is almost the same.

3.4. Simulation Result in the Indoor Arena with Three Obstacles

The simulated mobile robots using the proposed control strategies were tested in an obstacle-filled arena. We give a series of snap shots of the tracing odor plumes process of the six robots in the indoor arena with three obstacles (see Figure 9). At the beginning, six robots (indicated by "○") and a virtual robot (indicated by "+") are distributed randomly in the entrance area. At the time t=110s (see Figure 9(a)), some of the robots detected obstacle 2 within their sensor range, then they detoured around the obstacle 2 and continued plum-tracing with the wall-following collision avoidance force defined in (9) (see Figure 9(b)). At last, the robots find the source and the search is end (see Figure 9(c)).

Figure 10 and Figure 11 show the search results with the different number of robots *n* in the indoor arena with three obstacles.

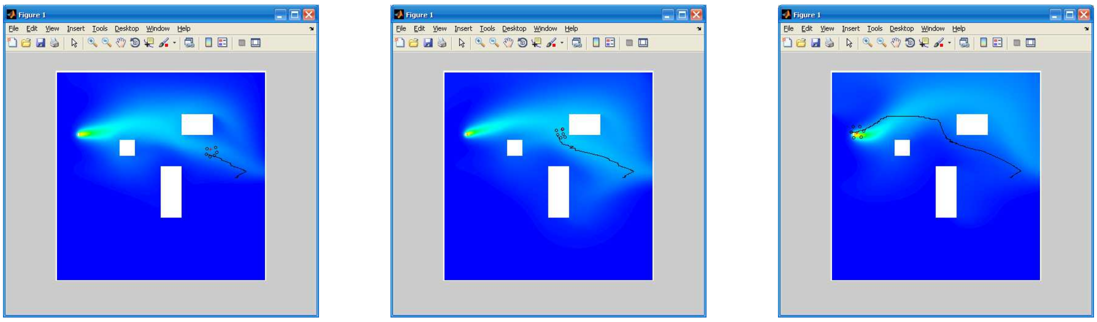

(a) t=110s (b) t=200s (c) t=412s

Figure 9. The virtual physics-based plume tracing process in indoor arena with three obstacles

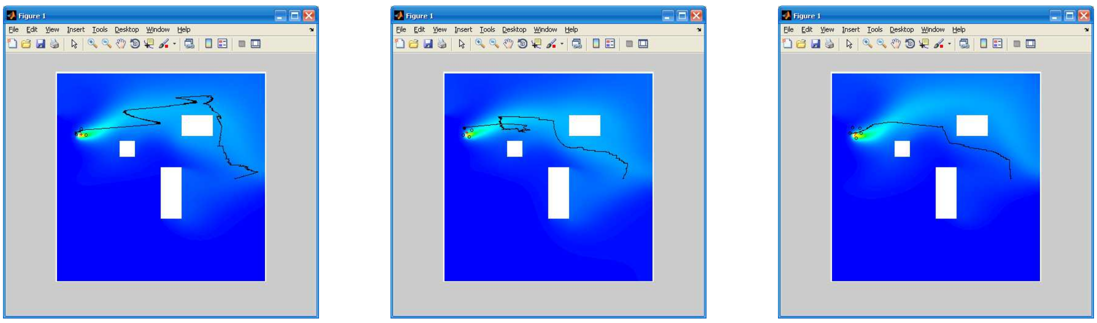

(a) *n*=3 (b) *n*=4 (c) *n*=5

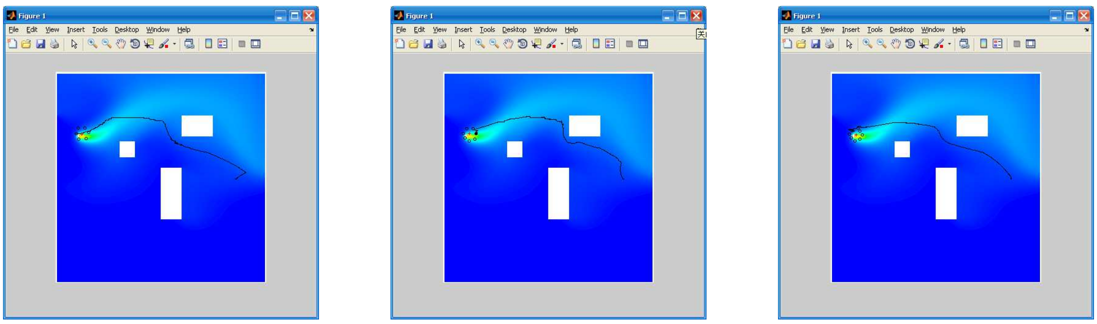

(d) *n*=6 (e) *n*=7 (f) *n*=8

Figure 10. Plume tracing path using the virtual physics in indoor arena with three obstacle with different robot number *n*

Figure 10 gives a tracing path of one of the robots and Figure 11 shows the search time and the overall proximity of the robots.

From Figure 10 and Figure 11 we can see, the obstacles make the distribution of the plume more diversified, so the search time in obstacles arena is much longer than it in no obstacle arena. The same as Figure 8, when the robot number is smaller, the search time of the robots is longer, while when the robot number is more than 4, the tracing path of the robots is very similar to each other with different robot number *n* and the search time is almost the same.

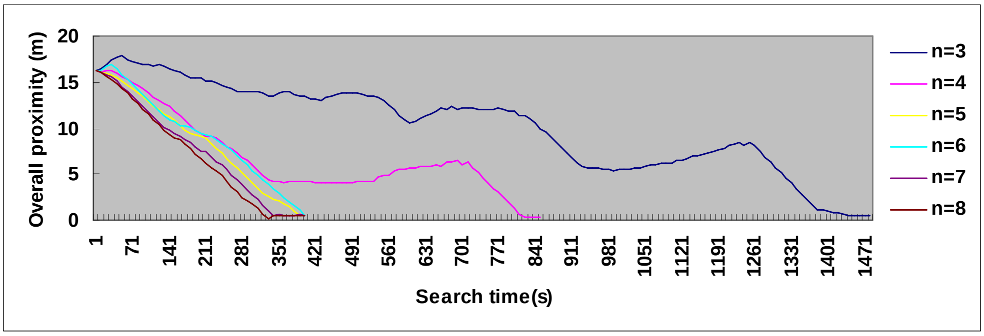

Figure 11. The performance of plume tracing using the virtual physics in indoor arena without obstacle with different robot number n

4. Conclusion

Odor source localization using multi-robots mainly includes the following aspects: the first is information sharing and behavioral integration among the robots. Second is the motion strategy of the robots, namely, which directions do the robots move toward? Finally is how to declare the odor source. This paper presents a cooperative search strategy based on mobile robotics swarms with virtual-physics force. The control force includes three kinds of effort, which are structure formation force, goal force, and obstacle avoidant force. With the virtual-physics forces, robots maintain the regular polygon formation while moving toward the chemical source in the indoor simulation arena. For swarm formation, a virtual robot is located at the center of the polygon. The innovative contribution of the strategy is that robots only having two kinds of force: structure formation force and obstacle avoidant force while virtual robot having only one kind of force: goal force. The motion of the virtual robot depends on the goal force which obtained from the sensor observations of robots. Once the virtual robot moved to a new place, robots would also move with the structure formation force and the obstacle avoidant force as a single body. The proposed strategy is simple, less parameters and easy to achieve. Simulation experiments in a no obstacle indoor arena and an obstacles contained indoor arena were carried out, and the results show that the proposed strategy can effectively navigate the mobile robotics swarms to the chemical source with proper robot number. At the same time, we discussed the influence of the number of the robots *n* to the search performance. The results tell us that considering the equipment cost of the robot platforms and the search performance; we suggest that the optimal number of robots in this paper should be five or six. Since hexagonal tiles can tile a planar region (i.e., the hexagonal grids can be connected without spatial gaps), this geometry is particularly well suited for sensor applications. So In the future, we will choose 6 robots composed of hexagonal grids to odor source localization in the more complex environment and further, transplant the control strategy on the true swam robots in the experiment arena.

Acknowledgements

This work was financially supported by the National Natural Science Foundation of China under Grant 60974126.

References

[1] Farrell JA, Pang S, Li W, Arrieta RM. *Biologically Inspired Chemical Plume Tracing on an Autonomous Underwater Vehicle*. Proceedings of the IEEE International Conference on Systems, Man and Cybernetics. Hague. 2004: 5991-5996.

[2] Sandini G, Lucarini G, Varoli M. *Gradient Driven Self-Organizing Systems*. Proceedings of the IEEE/RSJ International Conference on Intelligent Robots and Systems. Yokohama. 1993: 429-432.

[3] Dhariwal A, Sukhatme S, Aristides AG. *Bacterium-Inspired Robots for Environmental Monitoring*. Proceedings of the IEEE International Conference on Robotics and Automation. New Orleans, LA. 2004; 2: 1436-1443.

[4] Grasso F, Basil J, Atema J. *Towards the Convergence: Robot and Lobster Perspectives of Tracking Odors to their Source in the Turbulent Marine Environments*. Proceedings of the IEEE ISIC/CIRA/ISAS Joint Conference. Gaithersburg, MD. 1998: 259-263.

[5] Farrell JA, Pang S, Li W. Plume mapping via hidden markov methods. *IEEE Transactions on Systems, Man and Cybernetics-Part B, Cybernetics*. 2003; 33(6): 850-863.

[6] LI JG, MENG QH, LI F, Jiang P, Zeng M. Tracing Odor Plume by Robot in Time-variant Flow-field Environments. *Acta automatica sincia*. 2009; 10: 1327-1333.

[7] Jatmiko W, Mursanto P, Kusumoputro B. Modified PSO algorithm based on flow of wind for odor source localization problems in dynamic environments. *WSEAS Transactions on Systems.* 2008; 7(3): 106-113.

[8] Zhang YL, Ma XP, Miao YZ. *Localization of Multiple Odor Sources using Modified Glowworm Swarm Optimization with Collective Robots*. Proceedings of the 2011 Chinese Control Conference. Yantai. 2011: 1899-1904.

[9] Marques L, Nunes U, de Almeida AT. *Odour searching with autonomous mobile robots, an evolutionary-based approach*. Proceedings of IEEE International Conference on Advanced Robotics. Coimbra, Portugal. 2003: 494-500.

[10] Li JC, Meng QH, Liang Q. Simulation Study on Robot Active Olfaction Based on Evolutionary Gradient Search. *Robot*. 2007; 29(3): 234-238.

[11] Li W, Farrell JA, Pang S, et al. Moth-inspired chemical plume tracing on an autonomous underwater vehicle. IEEE Transactions on robotics. 2006; 22(2): 292-306

[12] Jiang P, Meng QH, Zeng M, et al. Indoor gas source identification by fusing visual and olfactory information of a mobile robot. *Chinese High Technology Letters.* 2011; 21(8): 867-873.

[13] Zarzhitsky D, Spears D, Spears W. *Distributed robotics approach to chemical plume tracing*. Proceedings of IEEE/RSJ international conference on intelligent robots and systems. Alberta. 2005: 4034-4039.

[14] Hayes AT, Martinoli A, Goodman RM. Distributed odor source localization. *IEEE Sensors Journal*. 2002; 2(3): 260-271.

[15] Cui X, Hardin CT, Ragade RK, Elmaghraby AS. *A Swarm approach for emission sources localization*. Proceedings of the 16th International Conference on Tools with Artificial Intelligence (ICTAI 2004). Boca Raton, Florida. 2004: 424-430.

[16] Jatmiko W, Sekiyama K, Fukuda T. *A Mobile Robots PSO-based for Odor Source Localization in Dynamic Environment Advection-Diffusion Environment*. Proceedings of the IEEE/RSJ International Conference on Intelligent Robotics and Systems. Beijing. 2006: 4527-4532.

[17] Liu ZZ, Lu TF. *A simulation framework for plume-tracing research*. Proceedings of the 2008 Australian Conference on Robotics & Automation. Canberra. 2008: 1-7.

[18] Rezaee H, Abdollahi F. *Mobile robots cooperative control and obstacle avoidance using potential field*. Proceedings of the 2011 IEEE/ASME International Conference on Advanced Intelligent Mechatronics. Budapest. 2011: 61-66.